Article ID: 1000-324X(2021)02-0210-07 **DOI:** 10.15541/jim20200143

Fabrication and Optical Property of Nd:Lu_2O_3 Transparent Ceramics for Solid-state Laser Applications

LIU Ziyu[1,2], TOCI Guido[3], PIRRI Angela[4], PATRIZI Barbara[3], FENG Yagang[1,2], CHEN Xiaopu[1,2], HU Dianjun[1,2], TIAN Feng[1,2], WU Lexiang[1], VANNINI Matteo[3], LI Jiang[1,2]

(1. Key Laboratory of Transparent Opto-functional Inorganic Materials, Shanghai Institute of Ceramics, Chinese Academy of Sciences, Shanghai 201899, China; 2. Center of Materials Science and Optoelectronic Engineering, University of Chinese Academy of Sciences, Beijing 100049, China; 3. Istituto Nazionale di Ottica, Consiglio Nazionale delle Ricerche, CNR-INO, Via Madonna del Piano 10C, 50019 Sesto Fiorentino (Fi), Italy; 4. Istituto di Fisica Applicata "Carrara", Consiglio Nazionale delle Ricerche, CNR-IFAC, Via Madonna del Piano 10C, 50019 Sesto Fiorentino (Fi), Italy)

Abstract: Nd^{3+} doped Lu_2O_3 crystal has been suggested to be potential gain medium for high-power solid-state lasers due to the high thermal conductivity, low phonon energy and excellent optical properties. Because of the extremely high melting point of above 2400 ℃, great attention has been paid to the Lu_2O_3-based transparent ceramics considering the comparable optical properties and laser performance with single crystal. In this work, we aimed at fabricating highly transparent Nd:Lu_2O_3 ceramics and investigating the optical properties and laser performance. 1.0at%Nd:Lu_2O_3 ceramics were fabricated by two-step sintering, namely vacuum sintering along with hot isostatic pressing (HIP) method, from coprecipitated nano-powders. The microstructures of the as-prepared powder, green body and ceramics were studied. The average grain size of the HIPed ceramics is 724.2 nm. The final ceramic sample has the in-line transmittance of 82.4% at 1100 nm (1.0 mm thickness). The absorption cross-section of 1.0at%Nd:Lu_2O_3 ceramics at 806 nm is 1.50×10^{-20} cm^2 and the calculated emission cross-section from fluorescence spectrum at 1080 nm is about 6.5×10^{-20} cm^2. The mean fluorescence lifetime, 169 μs, of the $^4F_{3/2}\rightarrow{}^4I_{11/2}$ was measured at the two excitation wavelengths of 878.8 and 895.6 nm, respectively. Laser performance of the annealed ceramic sample was investigated in quasi-continuous wave (QCW) condition. A maximum laser output power of 0.47 W with a slope efficiency of 8.7% is obtained by using an output coupler with a transmission of T_{OC}=2.0%. Briefly, laser level Nd:Lu_2O_3 transparent ceramics with high optical transparency and uniform microstructure have been fabricated, which are promising gain media for solid-state lasers.

Key words: Nd:Lu_2O_3 transparent ceramics; co-precipitation; two-step sintering; optical property; laser performance

Considerable attention has been paid to high power solid-state lasers due to their extensive applications in many fields, such as military, industry, scientific research and medical treatments[1-5]. As an active ion for laser gain materials, the Nd^{3+} is widely used in high power solid-state lasers. It has a typical four-level structure, which is advantageous for reducing the pump threshold and improving the efficiency as compared to the three-level system[6-7]. Moreover, the various f-shell transitions of Nd^{3+} ion enable these gain media to produce abundant laser emission lines[8-9]. Generally, the electrons of Nd^{3+} are excited to the level of $^4F_{5/2}$ after absorbing the pump light and then radiate spontaneously to the level of $^4F_{3/2}$. Subsequently, they can jump to four possible states from $^4F_{3/2}$, namely, $^4F_{3/2}\rightarrow{}^4I_{9/2}$, $^4I_{1F1/2}$, $^4I_{13/2}$, $^4I_{15/2}$, respectively[10]. Due to the availability of several transitions, Nd^{3+} doped materials can achieve single-wavelength, dual-wavelength or multi-wavelength laser output by

Received date: 2020-03-23; **Revised date:** 2020-04-28; **Published online:** 2020-06-15
Foundation item: National Key R&D Program of China (2017YFB0310500); Key Research Project of the Frontier Science of the Chinese Academy of Sciences (QYZDB-SSW-JSC022)
Biography: LIU Ziyu (1991–), female, PhD candidate. E-mail: liuziyu@student.sic.ac.cn
刘子玉(1991–), 女, 博士研究生. E-mail: liuziyu@student.sic.ac.cn
Corresponding author: LI Jiang, professor. E-mail: lijiang@mail.sic.ac.cn
李 江, 研究员. E-mail: lijiang@mail.sic.ac.cn

certain design[11-15].

Yttrium aluminum garnet (YAG) is the most widely used host for high power solid-state lasers because of the excellent optical, chemical and mechanical properties[16-19]. But higher thermal conductivity favors the heat transporting which is conducive to reduce thermal effects, and allows using higher pump power densities on gain media for high power lasers[20-21]. Therefore, sesquioxides host materials such as Lu_2O_3[22], Sc_2O_3[23] and Y_2O_3[24] have aroused extensive attention due to the higher thermal conductivity. An attractive feature of Nd^{3+}-doped sesquioxides gain media is that they have various emission lines in the near infrared region[10,25]. In particular, Lu_2O_3 appears especially promising because of the close ionic radius and mass match of Lu^{3+} to many lanthanide dopant ions of interest which support high doping levels with minimal sacrifice of thermal conductivity[26]. Moreover, Nd^{3+}-doped Lu_2O_3 gain medium has larger emission cross section ratio between 0.9 and 1.08 μm, and higher quantum efficiency than those of Nd:YAG[9,27]. Besides, it is easy for Nd:Lu_2O_3 crystal to operate in the dual-wavelength regime laser. The Nd:Lu_2O_3 pulsed laser operation was firstly achieved with the slope efficiency of 31%[28].

However, Lu_2O_3 has extremely high melting point (>2490 ℃) which hampers growing high-quality single crystals. In this respect, polycrystalline transparent ceramic materials appear as promising solid-state gain media especially for materials with high melting temperatures[29-30]. In 2002, laser-level Nd:Lu_2O_3 transparent ceramics were firstly fabricated by vacuum sintering from nano-powders, and 10 mW laser output was obtained with the maximum absorbed power of 185 mW[31]. Afterwards, various works have shown the fabrication of Nd:Lu_2O_3 transparent ceramics by spark plasma sintering (SPS) even realizing the maximum laser output to 1.25 W with a slope efficiency of 38%[30,32-34]. However, using graphite mould usually causes carbon contamination of ceramics in the SPS process. Generally it is more difficult for SPS to fabricate large-size laser transparent ceramics with uniform structures compared with other techniques such as vacuum sintering or HIP. As to vacuum sintering, it's almost impossible to remove all residual pores of transparent ceramics. While two-step sintering, namely vacuum sintering plus HIP post-treatment, can efficiently reduce the optical scattering loss of ceramics[35].

In this work, 1.0at%Nd:Lu_2O_3 ceramics were obtained by two-step sintering from co-precipitated nano-powder. We also investigated the microstructures, optical properties and laser performance of Nd:Lu_2O_3 ceramics systematically.

1 Experimental

Commercial oxide powders of Lu_2O_3 (99.999%, Zhongkai New Materials Co., Ltd., Jining, China) and Nd_2O_3 (99.99%, Alfa Aesar) were utilized as raw materials. 1.0at%Nd:Lu_2O_3 powder was synthesized by co-precipitation method with the optimized experimental results according to the reference [36]. The green bodies were pre-sintered at 1500 ℃ for 2 h plus HIP post-treatment at 1550 ℃ for 3 h under 150 MPa in Ar. Then final ceramics were annealed at 900 ℃ for 30 h in air, and polished to 1.0 mm thickness for further optical characterizations and laser test.

The specific surface area (S_{BET}) of the nano-powder was measured with the nitrogen adsorption method (BET, Quadrasorb SI, Micromeritics, USA). The phases of the precursor and powder were identified by the X-ray diffractometer (XRD, D/max2200 PC, Rigaku, Japan) with Cu Kα_1 radiation (λ=0.15418 nm) at a scanning rate of 5 (°)/min in the 2θ. The morphologies of the resultant precursor and the powder, the microstructures of the thermally etched surfaces of the pre-sintered and the final ceramics were observed by the field emission scanning electron microscope (FESEM, SU8220, Hitachi, Japan). In-line transmittance and absorption spectrum of the double-sided polished ceramic, 1.0 mm of thickness, were evaluated by the UV-VIS-NIR spectrophotometer (Cary-5000, Varian, USA). The fluorescence spectrum at room temperature was performed with the fluorescence spectrometer (FLS-980, EI, England).

2 Results and discussion

It can be seen from Fig. 1 that the XRD pattern of precursor includes amorphous diffraction peaks and a few obvious crystalline peaks approximately centered at an angle 2θ of 10.4°,19.8° and 32.7°. These peaks are possibly ascribed to the carbonates, indicating that the precursor may consist of mixtures of carbonates. After calcination at 1100 ℃ for 4 h, the phase of precursor transforms into pure phase of cubic Lu_2O_3. The average grain size (D_{XRD}) of 1.0at%Nd:Lu_2O_3 powder is about 60.8 nm, which is calculated from the XRD spectrum by the Scherrer's formula[37]:

$$D_{XRD} = 0.89\lambda / (\beta \cdot \cos\theta) \quad (1)$$

Where λ is the wavelength of Cu Kα1 radiation, and β is the full width at half-maximum (FWHM) of a diffraction peak at Bragg angle θ. The theoretical density ρ of the calcined powder is about 9.37 g/cm^3 according to the XRD result.

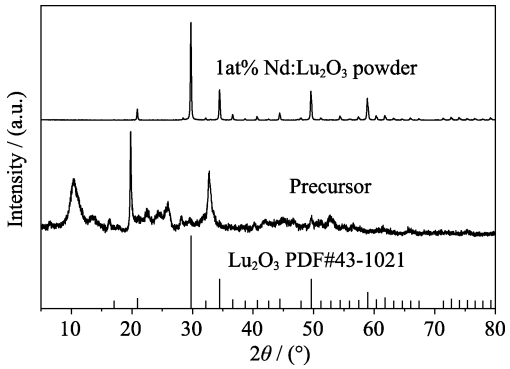

Fig. 1 XRD patterns of the as-synthesized precursor and 1.0at%Nd:Lu_2O_3 powder calcined at 1100 ℃ for 4 h

The FESEM micrographs of the precursor, calcined powder and green body are shown in Fig. 2. The precursor has a 2-D loosely lamellar structure with a thickness of several tens nanometers, as it appears from Fig. 2(a). The mixtures of carbonates decompose into oxides after being calcined at 1100 ℃ for 4 h. It is clear that a small amount of lamellar structures still can be found and the powder consists of nanoparticles, as shown in Fig. 2(b). The average particle size (D_{BET}) can be obtained from the specific surface area (S_{BET}) of 8.254 m^2/g by the formula:

$$D_{BET} = 6/(\rho \cdot S_{BET}) \quad (2)$$

The calculated value is 77.6 nm. The agglomeration degree of the 1.0at%Nd:Lu_2O_3 powder can be estimated by the $(D_{BET}/D_{XRD})^3$ of 2.16, indicating that the dispersity of powder still need to be improved. Firstly, the loose powder was uniaxially pressed into a disk with a diameter of 18 mm under 69 MPa. Subsequently, the green bodies were formed by cold isostatic pressing (CIP), with a relative density of 51.2%. As can be seen from Fig. 2(c), the green body is relatively compact with uniform structures, which is favorable for the fabrication of highly transparent ceramics. This also shows that dry pressing could effectively break the lamellar powder.

The green bodies were pre-sintered at 1500 ℃ for 2 h in vacuum without pressure. The pre-sintered ceramics are opaque after mirror-polishing. They do not possess completely dense microstructures, and their relative density measured by the Archimedes method is 96.7%. It can be seen from the thermally etched surface of pre-sintered ceramics shown in Fig. 3(a) that there are still a large number of micro-pores located mostly at the grain boundaries. Because of the large number of pores, there is a strong light scattering in the pre-sintered ceramics to cause the opaque. However, the double-sided polished ceramics are highly transparent after HIP post-treatment at 1550 ℃ for 3 h under 150 MPa in Ar. Apparently, no evident micro-pores can be observed, and the thermally etched HIPed ceramic sample is nearly fully dense as shown in Fig. 3(b). The average grain size of the HIPed sample is 724.2 nm with just a little growth compared to that of the pre-sintered one (646.7 nm), which are obtained by the linear intercept method. The microstructure shown in Fig. 3(b) appears to be uniform.

The HIPed ceramics were annealed at 900 ℃ for 30 h and subsequently double-sided polished at laser grade with the thickness of 1.0 mm. The sample has relatively high optical quality ranging from the visible to infrared wavelength, with the in-line transmittance of 82.4% at 1100 nm and 78.3% at 400 nm, as shown in Fig. 4. The decreasing transmittance in short wavelength region may be ascribed to the tiny pores. Some residual pores of pre-sintered ceramics are removed while the rest are possibly compressed into tiny pores during the HIP process. In order to remove these residual pores in final ceramics as many as possible, the experimental parameters during the two-step sintering process are worth exploring in the following work.

Fig. 5 shows the room-temperature absorption cross section (σ_{abs}) spectrum of 1.0at%Nd:Lu_2O_3 transparent ceramics in the wavelength range from 200 to 1000 nm, which can be calculated from the absorption coefficient by:

$$\alpha = \frac{-2.303\lg(I/I_0)}{L} \quad (3)$$

$$\sigma_{abs} = \frac{\alpha}{N} \quad (4)$$

Where α is the absorption coefficient, $\lg(I/I_0)$ is the optical density obtained by the spectrophotometer, L is the thickness of the ceramics and N is the number of the doping ions in the unit volume. The value of N is

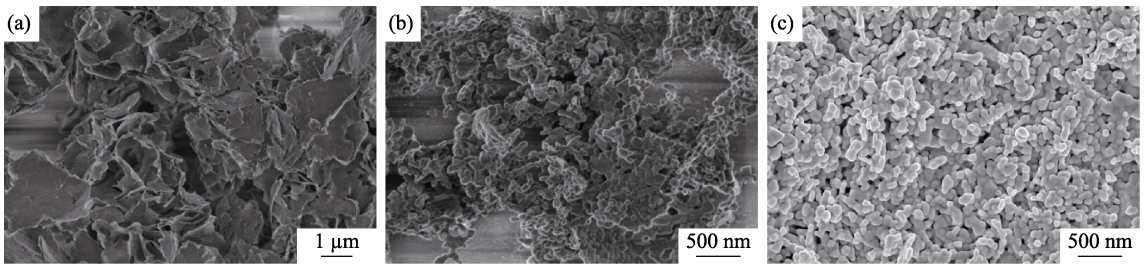

Fig. 2 FESEM micrographs of (a) precursor, (b) 1.0at%Nd:Lu_2O_3 powder and (c) green body formed from the nano-powder

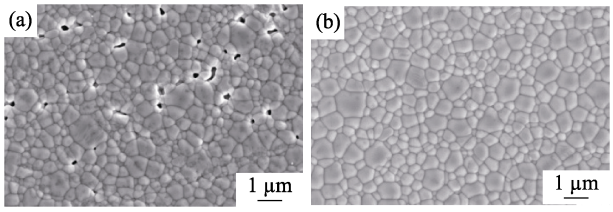

Fig. 3　FESEM micrographs of the thermally etched (1300 ℃ for 3 h) surfaces of 1.0at%Nd:Lu_2O_3 ceramics
(a) Ceramic pre-sintered at 1500 ℃ for 2 h; (b) Ceramic HIP post-treated at 1550 ℃ for 3 h

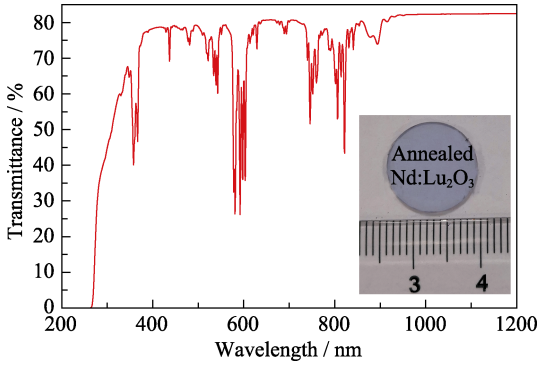

Fig. 4　In-line transmittance and the photograph of the double-side polished 1.0at%Nd:Lu_2O_3 transparent ceramics

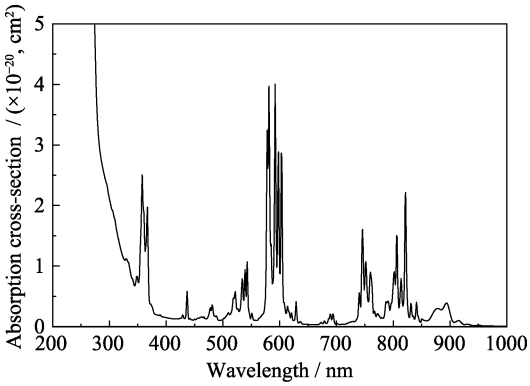

Fig. 5　Room-temperature absorption cross-section spectrum of the 1.0at%Nd:Lu_2O_3 ceramics annealed at 900 ℃ for 30 h

2.84×10^{20} ions/cm^3 for 1.0at%Nd:Lu_2O_3 ceramic sample. It shows several different absorption bands around 358, 437, 481, 521, 543, 592, 694, 746, 806, 822 and 894 nm, respectively, which are assigned to spin- or electric-dipole-allowed transitions from the ground state ($^4I_{9/2}$) to $^4D_{3/2}$, $^2P_{1/2}$, $^2G_{11/2}$+$^2P_{3/2}$+$^2D_{3/2}$+$^2G_{9/2}$, $^4G_{9/2}$, $^4G_{7/2}$, $^4G_{5/2}$, $^4F_{9/2}$, $^4F_{7/2}$+$^4S_{3/2}$, $^2H_{9/2}$,$^4F_{5/2}$ and $^4F_{3/2}$ energy levels, respectively[2]. The absorption cross-section at 806 nm is 1.50×10^{-20} cm^2.

Fig. 6(a) shows the room-temperature fluorescence spectrum of the annealed 1.0at%Nd:Lu_2O_3 ceramics under excitation at 808 nm by laser-diode (LD) source. It can be seen that two strongest fluorescence peaks locate at 1080 and 1076 nm, respectively, corresponding to the transition of $^4F_{3/2}\rightarrow{}^4I_{11/2}$. The stimulated emission

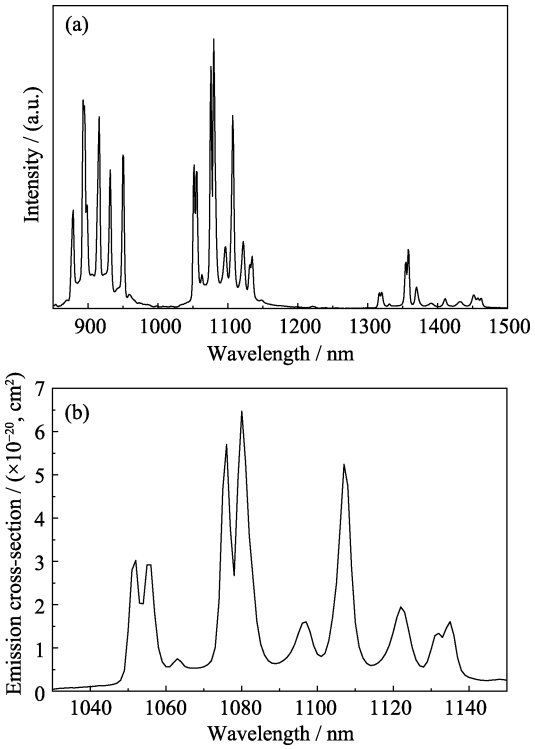

Fig. 6　(a) Room-temperature fluorescence spectrum and (b) emission cross-section of the 1.0at%Nd:Lu_2O_3 ceramics annealed at 900 ℃ for 30 h

cross-section could be evaluated by the Füchtbauer-Ladenburg formula:

$$\sigma(\lambda)=\frac{\lambda_{peak}^4\beta}{8\pi n^2 c\tau_{rad}}\cdot\frac{I(\lambda_{peak})}{\int I(\lambda)\,d\lambda} \tag{5}$$

$$n^2=D_1+\frac{D_2}{\lambda^2-D_3}-D_4\lambda^2 \tag{6}$$

Where λ is the wavelength in μm, β is the branching ratios of the transition of $^4F_{3/2}\rightarrow{}^4I_{11/2}$, $I(\lambda)$ is the intensity of the room-temperature fluorescence spectrum, n is the reflective index obtained by the Sellmeier equation in Ln^{3+}:Lu_2O_3 with D_1=3.61968, D_2=0.04131, D_3=0.00856[38] and τ_{rad} is the radiative lifetime of the upper laser level $^4F_{3/2}$. The theoretical value of τ_{rad} is 344 μs calculated by the Judd-Ofelt theory[10]. The calculated emission spectrum is shown in Fig. 6(b). The two strongest emission peaks of the $^4F_{3/2}\rightarrow{}^4I_{11/2}$ transition locate at 1076 and 1080 nm with the maximum emission cross-section at 1080 nm of about 6.5×10^{-20} cm^2.

The measurement of the upper level lifetime of 1.0at%Nd:Lu_2O_3 ceramics was carried out with the excitation radiation tuned either to 878.8 nm or 895.6 nm, respectively. These wavelengths correspond to the absorption of the $^4I_{9/2}\rightarrow{}^4F_{3/2}$ transition of electrons for Nd^{3+} in sites with C_2 symmetry, which is the most

important site for laser emission as the Nd^{3+} ions in the sites with C_{3i} symmetry have a small emission and absorption cross section[33]. The obtained fluorescence decay behaviors with excitation at the two different wavelengths are substantially identical, as it can be seen from the results shown in Fig. 7. The mean fluorescence lifetime can also be evaluated numerically with the following formula:

$$\tau_{\text{mean}} = \frac{1}{I(t=0)}\int_0^{\infty} I(t)\mathrm{d}t \qquad (7)$$

Where t is the excitation time. Using the Eq. (7), when the ceramic sample is respectively excited at 878.8 and 895.6 nm, we obtain the same value of the lifetime, τ_{mean}=169 μs. This value is relatively higher than the value of 153 μs measured for 1.0at%Nd:Lu_2O_3 ceramics from the reference [34], but substantially lower than the theoretical value of 344 μs calculated from J-O theory. It is also lower than the value of the single crystal[10]. This reduced lifetime may be addressed to the lattice defects and concentration quenching effect.

The laser test was performed using the laser cavity layout shown in Fig. 8, similar to that for Yb-doped materials[39]. The sample was soldered by a sheet of indium on a copper heat-sink and cooled by water at 17 ℃, and pumped by a fiber-coupled LD. It emits at 789.3 nm (FWHM 2.4 nm) with an almost cylindrical

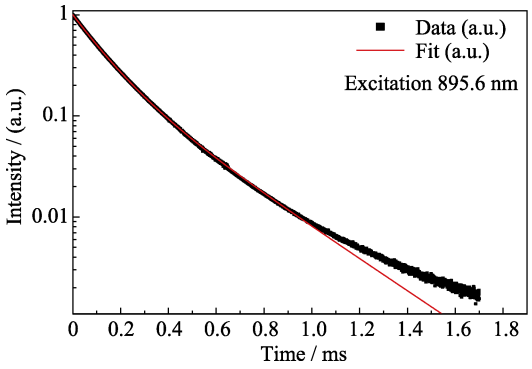

Fig. 7 Fluorescence decay of the 1.0at%Nd:Lu_2O_3 ceramics excited at two different wavelengths

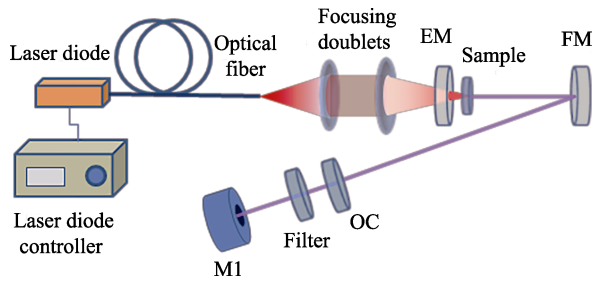

Fig. 8 Schematic of the laser cavity layout employed for the laser tests

intensity distribution in the region of the focal plane (*i.e.* beam radius 50 μm, measured with a CCD camera), and numerical aperture of the pump beam is 0.22. The resonator cavity consists of various optical elements such as End-Mirror (EM), Folding-Mirror (FM, spherical, ROC=150 mm) and Flat Output Coupler mirror (OC). Both EM and FM are dichroic (high transmission for the pump wavelength, high reflection between 980 and 1100 nm) and 80 mm apart. The distance between FM and OC is 137 mm. The output power is measured by the power meter M1, and a filter is used to reject the residual pump radiation, preventing it from reaching the power meter. The transmission of the filter at the lasing wavelength, *i.e.* 81.5%, was considered in the evaluation of the actual output power values.

The 1.0at%Nd:Lu_2O_3 ceramic sample was pumped in QCW mode (10 Hz of repetition rate, duty factor of DF=20%) in order to limit the thermal load into the ceramic sample. The maximum absorbed pump power by the sample was 5.9 W, corresponding to 33 W of incident pump power. Under lasing conditions, 18% of the incident pump power was absorbed by the sample. Laser output was successively extracted through OCs with different transmission values (T_{OC}=2.0%, 5.2%, 7.0%, 19.0%) to find the optimal output coupling transmission. The lasing wavelength was measured by a fiber-coupled spectrometer with a resolution of 0.4 nm along the entire wavelengths range.

Fig. 9(a) shows the output power as a function of the absorbed pump power for the 1.0at%Nd:Lu_2O_3 ceramic sample under test using output couplers with various transmission values. All main laser emission parameters are reported in Table 1. It can be seen that the laser threshold increases by increasing the transmission value of OC mirror. The slope efficiencies are similar for the OCs with transmission values ranging from 2.0% to 7.0%, whereas the maximum optical efficiency, that is 7.8%, was obtained by T_{OC}=2.0%. The slope efficiency and laser output power are higher than those of the Nd:Lu_2O_3 ceramics obtained by vacuum sintering[31]. However, the laser performance needs to be improved by further decreasing the optical loss of Nd:Lu_2O_3 ceramics.

Fig. 9(b) reports the two highest emission peaks acquire with 4.8 W of absorbed pump power when the cavity is closed with different OCs. The laser emits simultaneously on two different wavelengths respectively at 1076 nm and at 1080.3 nm, corresponding to the transition from the level $^4F_{3/2}$ to the $^4I_{11/2}$. It appears that the main emission peaks at about 1076 nm, with a fraction (between 20% and 30%) of emission peaking at 1080 nm.

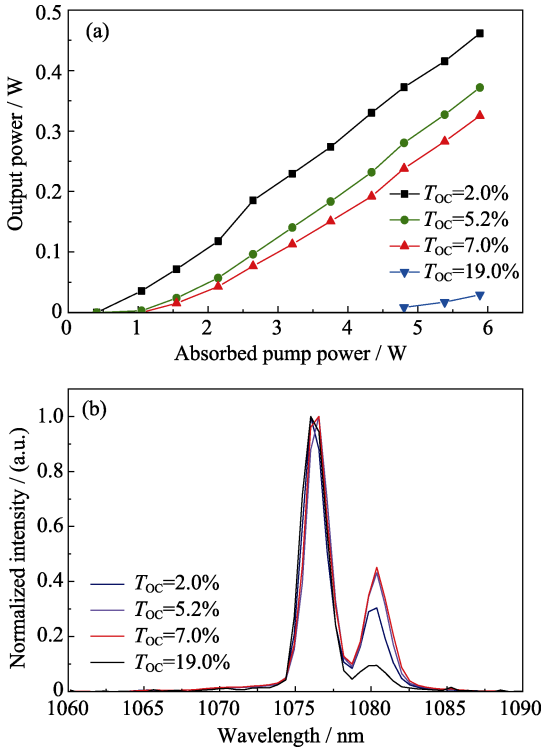

Fig. 9　Laser output power *vs* incident pump power (a) and emission spectra for different transmission values of the OC (b)

Table 1　Main laser emission parameters

Output coupler transmission/ %	Maximum power/ W	Slope efficiency/ %	Optical efficiency*/ %	Laser threshold/ W
2.0	0.460	8.7	7.8	0.57
5.2	0.372	8.9	6.3	0.81
7.0	0.325	8.3	5.7	1.20
19.0	0.029	1.9	0.5	4.42

*: Calculated with respect to the absorbed pump power

3　Conclusion

1.0at%Nd:Lu_2O_3 transparent ceramics were fabricated by vacuum sintering plus HIP methods from the co-precipitated nano-powder in this work. The microstructures of powder, green body and ceramics were studied in detail. The green bodies showed a relatively compact and uniform structure from the lamellar nano-powder. Porous ceramics pre-sintered in vacuum for short time finally turned into completely dense ceramics after HIP post-treatment. The in-line transmittance of 1.0at%Nd:Lu_2O_3 ceramics with the thickness of 1.0 mm was 82.4% at 1100 nm after annealing.

We also have systematically investigated the spectral properties and the laser performance of 1.0at%Nd:Lu_2O_3 ceramics. The ceramic sample showed many absorption bands due to the large number of f-shell transitions of Nd^{3+} ion and the absorption cross-section at 806 nm was 1.50×10^{-20} cm^2. The strongest two emission peaks of the $^4F_{3/2}\rightarrow{}^4I_{11/2}$ transition locating at 1076 and 1080 nm with the maximum emission cross-section at 1080 nm of about 6.5×10^{-20} cm^2, which was calculated from the fluorescence spectrum. The fluorescence lifetime of the upper level $^4F_{3/2}$ measured at the two excitation wavelengths of 878.8 or 895.6 nm was 169 μs, which is lower than the theoretical value. This was possibly ascribed to the lattice defects of Lu_2O_3 ceramics and the quenching of Nd^{3+} ions concentration. The ceramic sample was pumped in QCW with a maximum laser output power of 0.47 W corresponding to a slope efficiency of 8.7% (T_{OC}=2.0%). The tested laser performance demonstrated that the optical quality of Nd:Lu_2O_3 ceramics still remained to be improved, such as the microstructures, the optical uniformity and the surface quality of Nd:Lu_2O_3 ceramics, to reduce the optical loss.

References:

[1] IKESUE A, AUNG Y L. Ceramic laser materials. *Nature Photonics*, 2018, **2(12):** 721–727.
[2] KAMINSKII A A. Laser crystals and ceramics: recent advances. *Laser & Photonics Reviews*, 2007, **1(2):** 93–177.
[3] TAIRA T. RE^{3+}-ion-doped YAG ceramic lasers. *IEEE Journal of Selected Topics in Quantum Electronics*, 2007, **13(3):** 798–809.
[4] TAO X T, WANG S P, WANG L, *et al.* Research in crystal materials: from bulk crystals to micro-nano crystals. *Journal of Synthetic Crystals,* 2019, **48:** 765–785.
[5] LI N, LIU B, SHI J J, *et al*. Research progress of rare-earth doped laser crystals in visible region. *Journal of Inorganic Materials*, 2019, **34:** 573–589.
[6] GRUBER J B, SARDAR D K, YOW R M, *et al.* Energy-level structure and spectral analysis of Nd^{3+} ($4f^3$) in polycrystalline ceramic garnet $Y_3Al_5O_{12}$. *Journal of Applied Physics*, 2004, **96(6):** 3050–3056.
[7] LI J H, LIU X H, WU J B, *et al.* High-power diode-pumped Nd:Lu_2O_3 crystal continuouswave thin-disk laser at 1359 nm. *Laser Physics Letters*, 2012, **9(3):** 195–198.
[8] JU M, XIAO Y, ZHONG M M, *et al.* New theoretical insights into the crystal-field splitting and transition mechanism for Nd^{3+}-doped $Y_3Al_5O_{12}$. *ACS Applied Materials & Interfaces*, 2019, **11(11):** 10745–10750..
[9] BRUNN P V, HEUER A M, FORNASIERO L, *et al.* Efficient laser operation of Nd^{3+}:Lu_2O_3 at various wavelengths between 917 nm and 1463 nm. *Laser Physics*, 2016, **26(8):** 084003.
[10] HAO L Z, WU K, CONG H J, *et al.* Spectroscopy and laser performance of Nd:Lu_2O_3 crystal. *Optics Express*, 2011, **19(18):** 17774–17779.
[11] XUE X G, ZHANG F, ZHAO H Q. Influence of the Nd:YAG laser-induced color center absorption on 1064 nm laser output power. *Journal of Synthetic Crystals*, 2018, **47(5):** 1083–1088.
[12] PAVEL N. Simultaneous dual-wavelength emission at 0.90 and 1.06 μm in Nd-doped laser crystals. *Laser Physics*, 2010, **20(1):** 215–221.
[13] HUANG B, YI Q, YANG L L, *et al.* Dual-wavelength nanosecond Nd:YVO_4 laser with switchable inhomogeneous polarization output. *IEEE Journal of Selected Topics in Quantum Electronics*, 2018, **24(5):** 1–5.
[14] PANG S Y, QIAN X B, WU Q H, *et al*. Structure and spectral property of Sc doped Nd:CaF_2 laser crystals. *Journal of Inorganic Materials*, 2018, **33(8):** 873–876.
[15] DANAILOV M B, MILEV I Y. Simultaneous multiwavelength operation of Nd:YAG laser. *Applied Physics Letters*, 1992, **61(7):** 746–748.
[16] WANG Q Q, SHI Y, FENG Y G, *et al.* Li J. Spectral characteristics and laser parameters of solar pumped Cr,Nd:YAG transparent ceramics. *Chinese Journal of Luminescence*, 2019, **40(11):** 1365–1372.
[17] SANGHERA J, KIM W, VILLALOBOS G, *et al.* Ceramic laser materials: past and present. *Optical Materials*, 2013, **35:** 693–699.
[18] SPRINGER R M, THOMAS M E. Analysis and comparison of single crystal and polycrystalline Nd:YAG, absorption. *IEEE Journal of Quantum Electronics*, 2013, **49(8):** 667–676.

[19] WANG H M, HUANG Z Y, QI J Q, *et al*. A new methodology to obtain the fracture toughness of YAG transparent ceramics. *Journal of Advanced Ceramics*, 2019, **8:** 418–426.
[20] LAPUCCI A, VANNINI M, CIOFINI M, *et al.* Design and Characterization of Yb and Nd Doped Transparent Ceramics for High Power Laser Applications: Recent Advancements. XXI International Symposium on High Power Laser Systems and Applications, Gmunden, Austria, 2016, **10254:** 102540E.
[21] GARREC B L, CARDINALI V, BOURDET G. Thermo-optical Measurements of Ytterbium Doped Ceramics (Sc_2O_3, Y_2O_3, Lu_2O_3, YAG) and Crystals (YAG, CaF_2) at Cryogenic Temperatures. High-power, High-energy, and High-intensity Laser Technology; and Research Using Extreme Light: Entering New Frontiers with Petawatt-Class Lasers, 2013, **8780:** 87800E.
[22] LIU Q, LI J B, DAI J W, *et al.* Fabrication, microstructure and spectroscopic properties of Yb:Lu_2O_3 transparent ceramics from co-precipitated nanopowders. *Ceramics International*, 2018, **44(10):** 11635–11643.
[23] DAI Z F, LIU Q, TOCI G, *et al.* Fabrication and laser oscillation of Yb:Sc_2O_3 transparent ceramics from co-precipitated nano-powders. *Journal of the European Ceramic Society*, 2018, **38(4):** 1632–1638.
[24] BALLATO J, MCMILLEN C, KOKUOZ B, *et al.* The Synthesis and Properties of Rare Earth Doped Yttria and Scandia for Eye-safe Single Crystal and Ceramic Lasers. Solid State Lasers XVII: Technology and Devices, California, United States, 2008, **6871:** 68711G.
[25] WALSH B M, MCMAHON J M, EDWARDS W C, *et al.* Spectroscopic characterization of Nd:Y_2O_3: application toward a differential absorption lidar system for remote sensing of ozone. *JOSA B*, 2002, **19(12):** 2893–2903.
[26] MCMILLEN C D, SANJEEWA L D, MOORE C A, *et al.* Crystal growth and phase stability of Ln:Lu_2O_3 (Ln=Ce, Pr, Nd, Sm, Eu, Tb, Dy, Ho, Er, Tm, Yb) in a higher-temperature hydrothermal regime. *Journal of Crystal Growth*, 2016, **452:** 146–150.
[27] SINGH S, SMITH R G, VAN UITERT L G. Stimulated-emission cross section and fluorescent quantum efficiency of Nd^{3+} in yttrium aluminum garnet at room temperature. *Physical Review B*, 1974, **10(6):** 2566.
[28] WANG B L, YU H H, ZHANG H, *et al.* Topological insulator simultaneously Q-switched dual-wavelength Nd:Lu_2O_3 laser. *IEEE Photonics Journal*, 2014, **6(3):** 1–7.
[29] LI J, PAN Y B, ZENG Y P, *et al.* The history, development, and future prospects for laser ceramics: a review. *International Journal of Refractory Metals and Hard Materials*, 2013, **39:** 44–52.
[30] BOULESTEIX R, EPHERRE R, NOYAU S, *et al.* Highly transparent Nd:Lu_2O_3 ceramics obtained by coupling slip-casting and spark plasma sintering. *Scripta Materialia*, 2014, **75:** 54–57.
[31] LU J, TAKAICHI K, UEMATSU T, *et al.* Promising ceramic laser material: highly transparent Nd^{3+}:Lu_2O_3 ceramic. *Applied Physics Letters*, 2002, **81:** 4324–4326.
[32] XU C W, YANG C D, ZHANG H, *et al.* Efficient laser operation based on transparent Nd:Lu_2O_3 ceramic fabricated by spark plasma sintering. *Optics Express*, 2016, **24:** 20571–20579.
[33] ALOMBERT-GOGET G, GUYOT Y, GUZIK M, *et al.* Nd^{3+}-doped Lu_2O_3 transparent sesquioxide ceramics elaborated by the Spark Plasma Sintering (SPS) method. Part 1: Structural, thermal conductivity and spectroscopic characterization. *Optical Materials*, 2015, **41:** 3–11.
[34] TOCI G, VANNINI M, CIOFINI M, *et al.* Nd^{3+}-doped Lu_2O_3 transparent sesquioxide ceramics elaborated by the Spark Plasma Sintering (SPS) method. Part 2: First laser output results and comparison with Nd^{3+}-doped Lu_2O_3 and Nd^{3+}-Y_2O_3 ceramics elaborated by a conventional method. *Optical Materials,* 2015, **41:** 12–16.
[35] LEE S H, KUPP E R, STEVENSON A J, *et al*. Hot isostatic pressing of transparent Nd:YAG ceramics. *Journal of the American Ceramic Society*, 2009, **92:** 1456–1463.
[36] LIU Z Y, TOCI G, PIRRI A, *et al.* Fabrication and laser operation of Yb:Lu_2O_3 transparent ceramics from co-precipitated nano-powders. *Journal of the American Ceramic Society*, 2019, **102(12):** 7491–7499.
[37] PATTERSON A L. The Scherrer formula for X-ray particle size determination. *Physical Review*, 1939, **56(10):** 978.
[38] KAMINSKII A A, AKCHURIN M S, BECKER P, *et al.* Mechanical and optical properties of Lu_2O_3 host-ceramics for Ln^{3+} lasants. *Laser Physics Letters*, 2007, **5(4):** 300–303.
[39] FENG Y G, TOCI G, PIRRI A, *et al.* Fabrication, microstructure, and optical properties of Yb:$Y_3ScAl_4O_{12}$ transparent ceramics with different doping levels. *Journal of the American Ceramic Society*, 2020, **103(1):** 224–234.

固体激光用 Nd:Lu_2O_3 透明陶瓷的制备和光学性能研究

刘子玉[1,2], TOCI Guido[3], PIRRI Angela[4], PATRIZI Barbara[3], 冯亚刚[1,2], 陈肖朴[1,2], 胡殿君[1,2], 田 丰[1,2], 吴乐翔[1], VANNINI Matteo[3], 李 江[1,2]

(1. 中国科学院 上海硅酸盐研究所, 透明光功能无机材料重点实验室, 上海 201899; 2. 中国科学院大学, 材料与光电研究中心, 北京 100049; 3. 意大利国家研究委员会 国立光学研究所, 佛罗伦萨 50019; 4. 意大利国家研究委员会 "Carrara"应用物理研究所, 佛罗伦萨 50019)

摘 要: Nd:Lu_2O_3 材料由于具有高热导率、低声子能量和优异的光学特性而成为非常有前景的高功率固体激光器用的增益介质。但 Lu_2O_3 单晶的熔点超过 2400 ℃, 难以生长, 而 Lu_2O_3 陶瓷既能在低温下制备, 又具有与晶体相当的光学性质和激光性能从而备受关注。本研究制备了高透明的 Nd:Lu_2O_3 陶瓷并对其光学性质和激光性能进行探究。以共沉淀法制备的纳米粉体为原料, 采用真空烧结结合热等静压(HIP)两步烧结法制备了 1.0at%Nd:Lu_2O_3 透明陶瓷。对制备的粉体、素坯和陶瓷的微结构进行了表征: HIP 后处理的陶瓷平均晶粒尺寸是 724.2 nm。厚度为 1.0 mm 的 1.0at%Nd:Lu_2O_3 透明陶瓷在 1100 nm 处的直线透过率是 82.4%, 样品在 806 nm 处的吸收截面为 1.50×10^{-20} cm^2, 而根据荧光光谱计算得到的发射截面为 6.5×10^{-20} cm^2。分别在 878.8 和 895.6 nm 波长激发下, 1.0at%Nd:Lu_2O_3 透明陶瓷 $^4F_{3/2}\rightarrow{}^4I_{11/2}$ 跃迁的平均荧光寿命均为 169 μs。当输出耦合镜的透过率 T_{OC}=2.0%时, 退火后的 1.0at% Nd:Lu_2O_3 透明陶瓷获得了最大输出功率为 0.47 W 的准连续(QCW)激光输出, 斜率效率为 8.7%。本研究成功制备了显微结构均匀、高透明度的 1.0at%Nd:Lu_2O_3 陶瓷, 并展示了其在固体激光增益介质领域的广阔应用潜力。

关 键 词: Nd:Lu_2O_3 透明陶瓷; 共沉淀法; 两步烧结; 光学性能; 激光性能

中图分类号: TQ174 **文献标识码:** A